Improvements in Microstructure Homogenization and Mechanical Properties of Diffusion-Alloyed Steel Compact by the Addition of Cr-Containing Powders

M.W. WU, K.S. HWANG, H.S. HUANG, and K.S. NARASIMHAN

The use of diffusion-alloyed powders for fabricating powder metal parts, despite alleviating the segregation problem of the alloying elements while retaining good compressibility, still cannot attain homogeneous microstructure in as-sintered products. The presence of soft Ni-rich areas and pores causes poor mechanical properties compared to those of wrought steel counterparts. This study investigated the effects of adding 0.5 wt pct Cr, which was introduced in the 316L stainless steel powder form, on the microstructure and mechanical properties of diffusion-alloyed Fe-4Ni-1.5Cu-0.5Mo-0.5C (Metal Powder Industries Federation (MPIF) FD-0405) steels. The results show that weak Ni-rich areas were present in the Cr-free specimen when sintered at 1120 °C and 1250 °C. These areas were lean in carbon because of the strong repelling effect between Ni and C. With the addition of 316L powders, the Cr was uniformly distributed and helped eliminate the soft Ni-rich areas, particularly in specimens sintered at 1250 °C. The distribution of carbon also improved. With a more uniform distribution of Ni and C, and more homogeneous microstructure, which consisted mainly of bainite and martensite, the mechanical properties of the Fe-4Ni-1.5Cu-0.5Mo-0.5C diffusion alloy steels were improved significantly.

I. INTRODUCTION

THE primitive method of making powder metal (P/M) products consists of compacting mixed elemental powders, followed by sintering. This mixing method creates segregation problems during powder handling and compaction and thus causes inhomogeneous microstructure in sintered products. As a result, the dimensional control and mechanical properties of P/M parts are inadequate. An intuitive approach to solving this problem is to use prealloyed steel powders. However, the poor compressibility of the hard prealloyed powder has prohibited its wide application. Another alternative is to employ diffusion-alloyed powders, for which iron powders and alloying elemental powders are diffusion bonded together at low temperatures.[1–4] These powders alleviate the segregation problem while maintaining good compressibility. However, the as-sintered microstructure of this powder, while improved, is still not homogeneous, unless extremely long sintering times or high sintering temperatures are employed. For example, in Ni-containing Fe-4Ni-1.5Cu-0.5Mo-0.5C alloys, which are designated by the Metal Powder Industries Federation (MPIF) as FD-0405, many Ni-rich areas are still present when the industrial sintering practices are used.[1,2,4] They are mostly found in the surface regions of iron powders, and such ringlike structures are known as the signature of this alloy. These soft Ni-rich areas have been blamed for the facilitation of crack propagation during mechanical testing.[5,6,7]

The reason why Ni is difficult to homogenize is possibly that it has a slower diffusion rate in iron than those of other alloying elements, such as C, Mo, and Cr.[8] Moreover, Ni has poor affinity with carbon, compared to other popular alloying elements such as Cr and Mo.[9] Thus, it is likely that the carbon distribution will not be uniform either, when such Ni-rich areas are present. Due to the inhomogeneous alloying and microstructure, the full benefits of the alloy design for such diffusion-alloyed steel powders cannot be attained.[4] In view of these problems, a better understanding of the causes of the inhomogeneous microstructure and a new method for improvement are required.

Since Cr is a strong carbide former, which could change the chemical potential of carbon in Ni-rich phases, it is possible that the presence of Cr in Ni-rich areas would increase the carbon content inside and help carbon homogenization.[9] The reduction of the repelling effect between Ni and C, if proved to be true, may also help improve the distribution of Ni in the C-containing matrix. Moreover, Cr has a faster diffusion rate than Ni. This fulfills the prerequisite that Cr should be in the matrix prior to the formation of Ni-rich areas, if such hypotheses are correct. However, the use of Cr as an alloying element, which is a good strengthening element in wrought steels, is rare in powder metal parts. The difficulty comes from its high oxygen affinity.[10] Thus, low-dew-point and high-temperature sintering are required to prevent the oxidation of Cr.[11,12] This creates problems for regular powder metal industries. This problem can be alleviated by reducing the activity of Cr using Cr-containing prealloyed powders. Since 316L stainless steel powders contain 16 to 18 wt pct Cr and are usually readily available in most powder metal plants, they could serve as a source for Cr alloying.

M.W. WU, Graduate Student, and K.S. HWANG, Professor, are with the Department of Materials Science and Engineering, National Taiwan University, Taipei, 106, Taiwan, Republic of China. Contact e-mail: kshwang@ccms.ntu.edu.tw H.S. HUANG, Researcher, is with the Material and Chemical Research Laboratories, ITRI, Taiwan, Republic of China. K.S. NARASIMHAN, Vice President, Technology, is with Hoeganaes Corp., Cinnaminson, NJ 08077-2017.

Manuscript submitted November 7, 2005.

Because very limited research on understanding the cause of the uneven Ni distribution, not to mention the methods for improvement, has been reported, the objective of this study was thus to examine the effects of 316L stainless steel addition on the microstructure and mechanical properties of diffusion-alloyed FD-0405 P/M steels.

II. EXPERIMENTAL PROCEDURE

The base powder used in this study was diffusion-alloyed Fe-4Ni-1.5Cu-0.5Mo steel powder that conformed to the MPIF FD-0405 standard. For the addition of chromium, 3 wt pct 316L powder or 0.5 wt pct Cr was introduced during the mixing process. Table I shows the characteristics of these two powders. The diffusion-alloyed powder was designated as material A. The material that was admixed with 316L powder was designated as material B. The final compositions of materials A and B are listed in Table II. Both of these materials were mixed with 0.6 wt pct graphite powder and 0.75 wt pct ethylene bis-stearamide, which is a lubricant, in a V-cone mixer for 30 minutes. The admixed powder was compacted into tensile bars per MPIF standard 10 at a pressure of approximately 500 MPa. The green densities of the tensile bars were maintained at 6.85 g/cm^3. The debinding was carried out by holding the green specimens at 550 °C for 15 minutes to remove the lubricant. After debinding, these specimens were subsequently sintered at 1120 °C for 30 minutes or at 1250 °C for 1 hour in a tube furnace, followed by furnace cooling. Both debinding and sintering were performed in an atmosphere of 91 pct N_2-9 pct H_2. The dew point of the atmosphere was below −45 °C. The average cooling rate of the furnace was 0.1 °C/s in the temperature range of 900 °C to 300 °C.

Table I. The Characteristics of Diffusion-Alloyed Powder and 316L Stainless Steel Powder Used in This Study

Type	Diffusion Alloyed Powder	316L Stainless Steel Powder
Designation	Distaloy 4800A	PF-20F
Average particle size	D_{10} = 16.27 μm	D_{10} = 5.75 μm
(Laser scattering method)	D_{50} = 46.85 μm	D_{50} = 13.67 μm
	D_{90} = 100.21 μm	D_{90} = 27.42 μm
Tap density, g/cm^3	3.43	3.85
Apparent density, g/cm^3	3.02	NA
Theoretical density, g/cm^3	7.91	7.92
Flow Rate, s/50 g	27.5	NA
Composition		
Ni, wt pct	3.84	12.7
Mo, wt pct	0.5	2.1
Cu, wt pct	1.5	—
Cr, wt pct	—	16.46
C	0.01	0.025
O	0.13	0.307
Supplier	Hoeganaes Corp. (Cinnaminson, NJ)	Epson ATMIX (Aomori, Japan)

Table II. The Compositions of Materials A and B Used in This Study

Designation	Ni (Wt Pct)	Mo (Wt Pct)	Cu (Wt Pct)	Cr (Wt Pct)	C (Wt Pct)
A	3.84	0.50	1.50	—	0.60
B (A + 3 wt pct 316L)	4.22	0.56	1.50	0.49	0.58

The densities of the sintered specimens were measured using the Archimedes' method. Tensile tests were performed using a strain rate of 0.0224/min (MTS, AG-10TE, Shimadzu Co., Kyoto, Japan). The data reported were averages of eight specimens. For microstructure observations, sintered tensile bars were ground, polished, and etched with a mixed solution of 4 pct nital and 2 pct picral. The microstructure was examined under a scanning electron microscope (SEM, XL-30, Philips, Eindhoven, Holland) or a conventional optical microscope. An electron probe microanalyzer (EPMA, JEOL JXA-8600SX, Japan Electron Optics Ltd., Tokyo, Japan) was also used to investigate the distribution of the alloying elements. Since the Ni distribution was quite inhomogeneous, an electron backscattering diffraction analyzer (EBSD, FE-SEM, JSM-6500F, JEOL, Tokyo, Japan) was used to identify the structures of the unknown phases. To understand the evolution of phase changes during cooling, a continuous cooling transformation (CCT) graph was built by placing specimens in a dilatometer (SETSYS TMA16/18, SETRAM, Caluire, France), heated to 900 °C and then cooled with various cooling rates. The microhardness was measured using a Vickers hardness (MVK-E2, Akashi Co., Tokyo, Japan) tester and the load applied was 10 gf.

III. RESULTS AND DISCUSSION

A. *Mechanical Properties*

The mechanical properties of as-sintered materials A and B (material A + 316L) along with the densities are listed in Table III. The data show that after 30 minutes of sintering at 1120 °C, the tensile strength of material B was higher than that of material A, the plain diffusion-alloyed powder, by 14 pct. The hardness also increased from HRB 83 to HRB 88. However, the elongation decreased slightly. These changes could not be attributed to the small density differences, nor were these improvements caused by the carbon content, because material B had a higher hardness but a lower carbon content.

After 1250 °C sintering, the tensile strength of material B significantly increased. This material was again higher than material A, by 28 pct. The hardness of material B also increased to HRB 99, higher than the HRB 91 of material A. These improvements, caused by the 316L powder addition, were not attributed to the differences in density or carbon content, because all the numbers were very close. It was more likely that the increases in tensile strength and hardness were caused by the improvement in microstructure.

B. *Microstructure of Fe-4Ni-1.5Cu-0.5Mo-0.5C P/M Steels*

Figure 1 shows the typical microstructure of diffusion-alloyed Fe-4Ni-1.5Cu-0.5Mo-0.5C steels (material A)

Table III. The Measured Values Along with Standard Deviations of Density, Carbon Content, and Mechanical Properties of Materials A and B

Material	Sintering Temperature (°C)	Density (g/cm^3)	Carbon Content (Pct)	Hardness (HRB)	Tensile Strength (MPa)	Elongation (Pct)
A	1120	6.85 (0.02)	0.51 (0.01)	83 (3)	530 (13)	2.3 (0.3)
	1250	6.90 (0.01)	0.48 (0.01)	91 (4)	626 (11)	2.0 (0.3)
B	1120	6.86 (0.03)	0.48 (0.01)	88 (4)	603 (14)	1.9 (0.2)
	1250	6.93 (0.03)	0.45 (0.02)	99 (3)	801 (10)	1.5 (0.2)

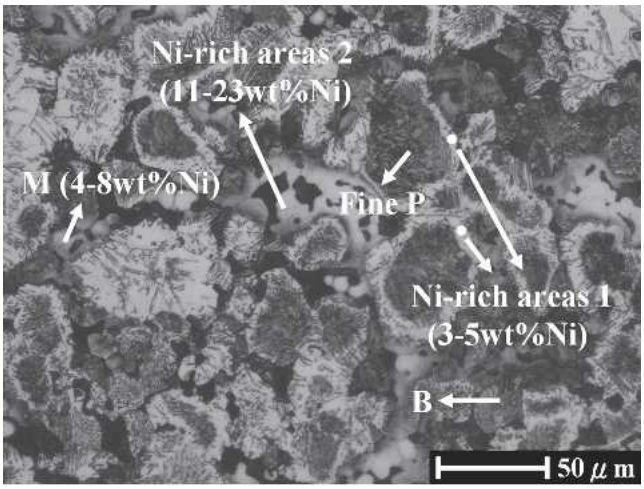

(*a*)

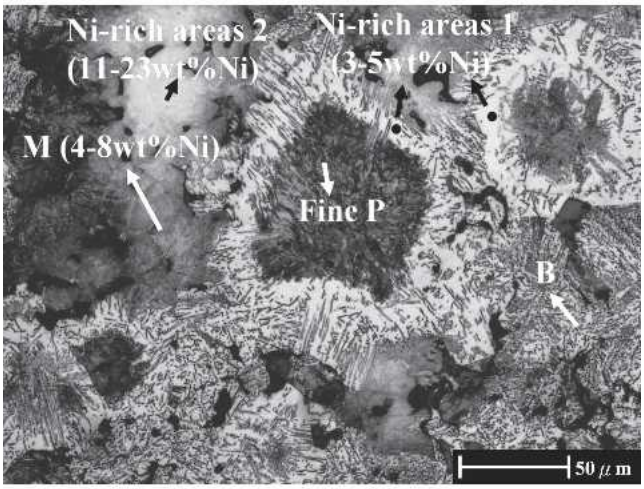

(*b*)

Fig. 1—The microstructure of the diffusion-alloyed Fe-4Ni-1.5Cu-0.5Mo-0.5C steel that was sintered at (*a*) 1120 °C for 30 min and (*b*) 1250°C for 1 h.

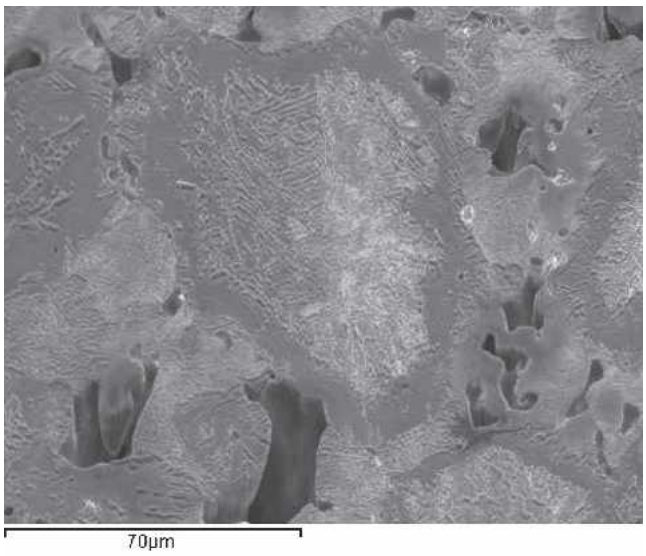

(*a*)

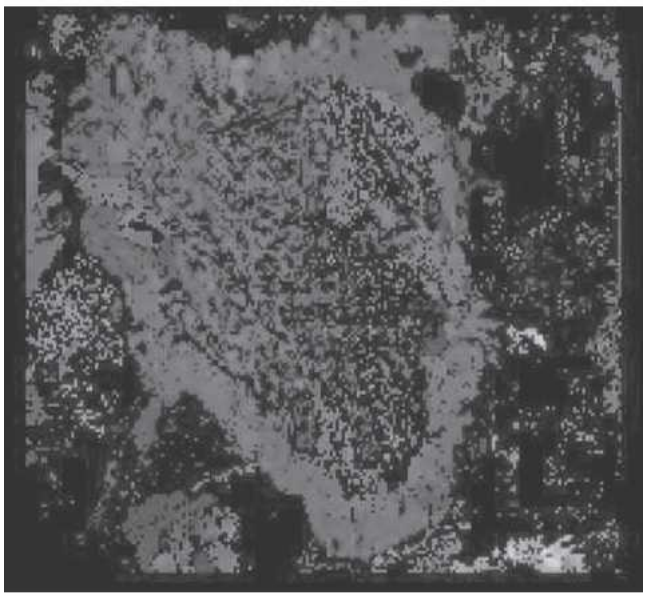

(*b*)

Fig. 2—The (*a*) microstructure and (*b*) EBSD mapping of Fe-4Ni-1.5Cu-0.5Mo-0.5C steels sintered at 1120 °C for 30 min showing that the powder periphery areas are ferrites.

after sintering at 1120 °C and 1250 °C. After 1120 °C sintering, the interior of the iron powder consisted mainly of pearlite, of which the Ni content was less than 0.1 wt pct, as measured by an EPMA. The hardness measured ranged from HV170 to HV250. In contrast, the areas at the periphery of the iron powders were enriched with 3 to 5 wt pct Ni and 1.5 wt pct Cu, and the hardness was only about HV140. Since no lamellae structures, such as those found in pearlite, and no featherlike structures, such as those found in bainite or martensite, were found, the microstructure, hardness, and composition of this area made us to believe that it is either ferrite or austenite. Since the phase identification for this powder periphery

area has not been reported in the literature, EBSD analysis was carried out. The mapping, as shown Figure 2, confirms that these soft powder periphery areas are ferrites.

It was also found that the pore-rich regions were enriched with Ni and Cu. However, these regions were not ferrites since they did not match the EBSD ferrite mapping. In areas that contained 4 to 8 wt pct Ni and 2 wt pct Cu, the hardness ranged between HV420 and HV562, similar to that of martensite. In other pore-rich areas, the hardness was low and ranged between HV170 and HV260. These soft areas contained 11 to 23 wt pct Ni and 4 wt pct Cu. It is believed that these areas were austenites because the high Ni and Cu content stabilized the austenitic structure down to the room temperature. The EPMA analysis also indicated that the carbon content in the soft Ni-rich area was lower than those in pearlite and martensite.[4] To facilitate the discussion of the soft Ni-rich areas, the soft area at the periphery of the iron powder was designated as Ni-rich area 1, while the soft pore-rich area was designated as Ni-rich area 2.

The inhomogeneity of the alloying was further verified by the mappings of Ni, Cu, and Mo. Figure 3 shows that molybdenum was uniformly distributed and that its content was between 0.4 and 0.6 wt pct, which was close to the nominal 0.5 pct. Since Mo could be easily homogenized, comparison of Mo mapping was neglected in the following sections. However, the Cu, Ni, and C distributions were nonuniform. It is believed that the Ni-rich areas were formed as a result of surface diffusion of Ni on the iron powders.[13,14,15] Most of the Ni remained near the surface, since its lattice diffusion rate into iron is quite slow. The Cu distribution was similar to that of Ni in that it covered the powder surfaces. This was because the copper melted during sintering and penetrated into the interparticle pores and powder contact areas due to the capillary force before it diffused inward to the powder core.[16–19] Since these Ni/Cu-rich and C-lean areas are low in hardness and their locations are in stress concentration regions, these areas could therefore be the most probable sites of crack initiation during mechanical testing.[6,7,20–22] However, further detailed experiments will be required to identify the phases

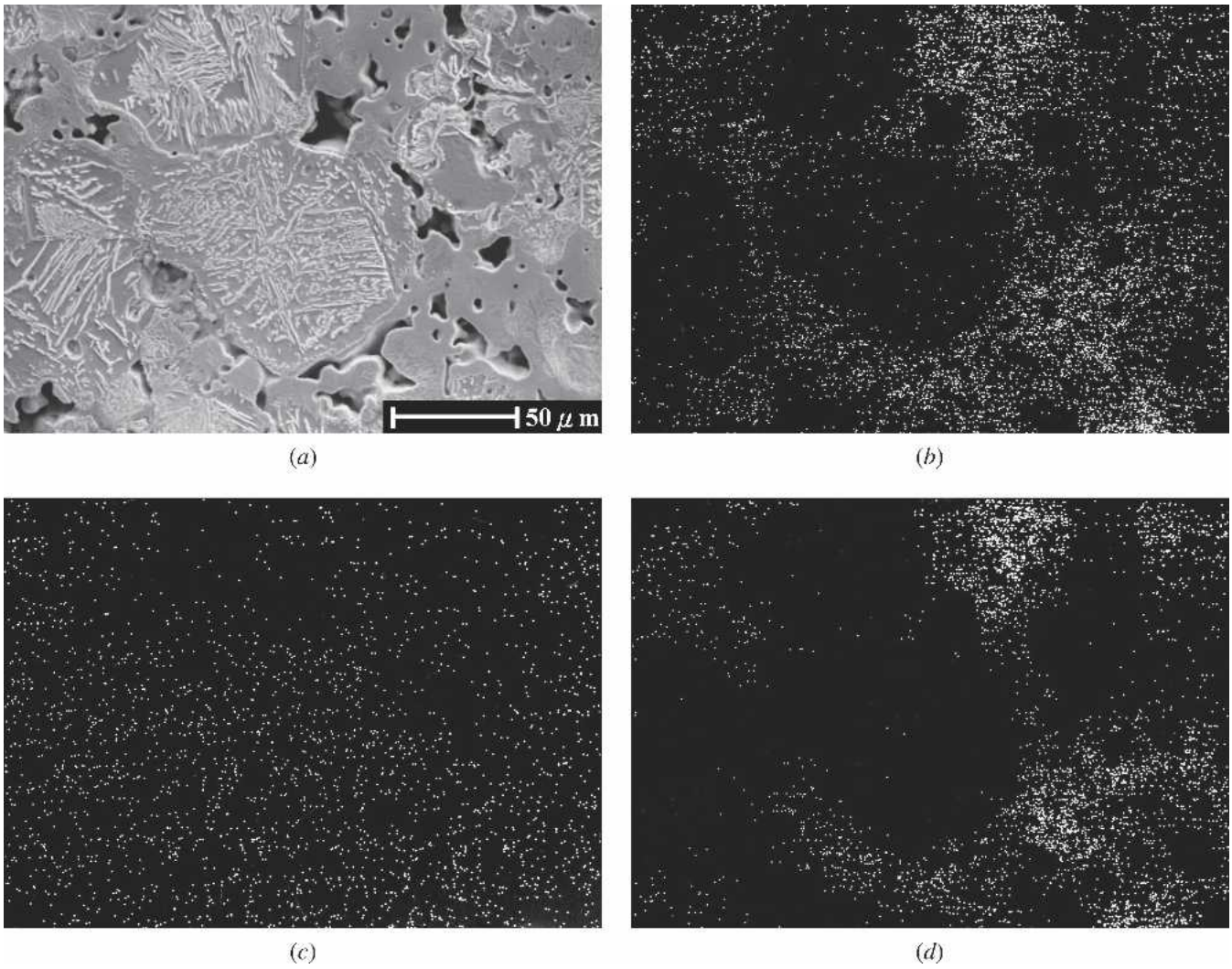

Fig. 3—(*a*) through (*d*) The Cu (*b*), Mo (*c*), and Ni (*d*) mappings of the diffusion-alloyed Fe-4Ni-1.5Cu-0.5Mo-0.5C specimen that was sintered at 1120 °C.

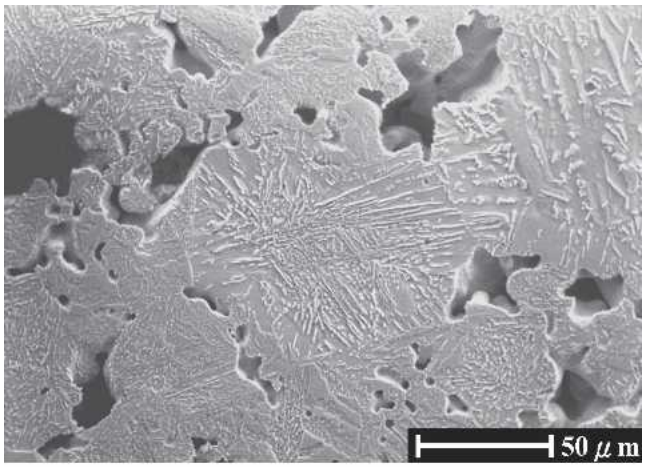

(*a*)

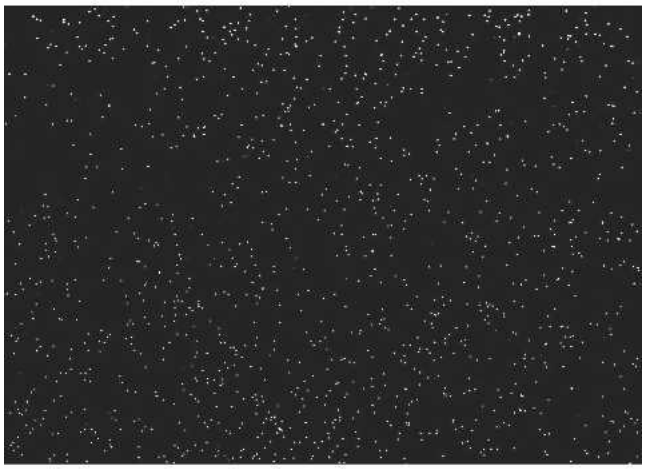

(*b*)

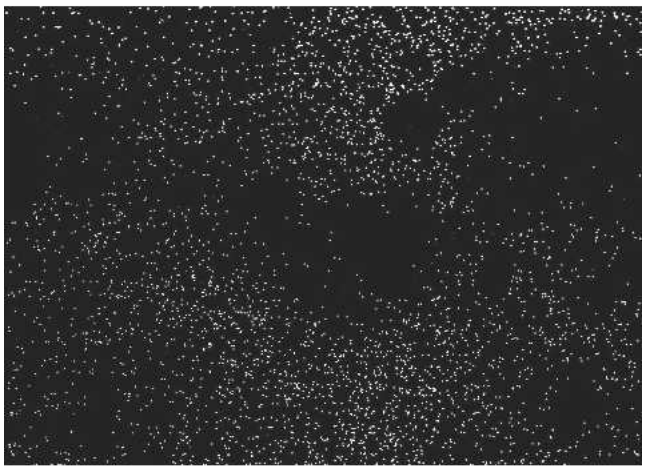

(*c*)

Fig. 4—(*a*) through (*c*) The Cu (*b*) and Ni (*c*) mappings of the diffusion-alloyed Fe-4Ni-1.5Cu-0.5Mo-0.5C specimen that was sintered at 1250 °C.

of these Ni/Cu rich areas and to correlate these phases with fracture behaviors.

When the sintering temperature increased to 1250 °C, the microstructure homogeneity improved significantly.

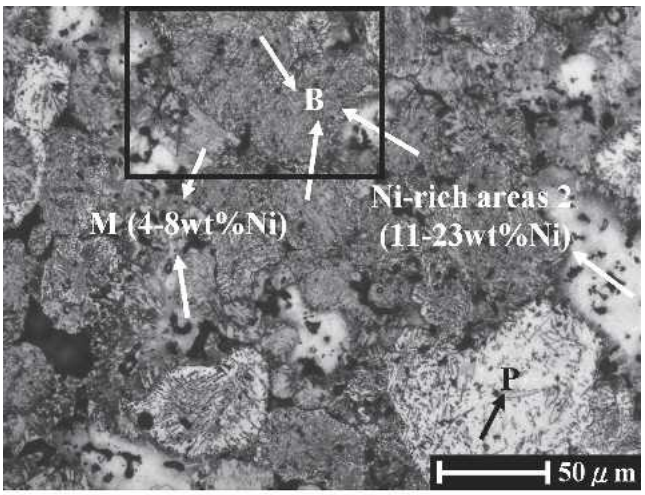

(*a*)

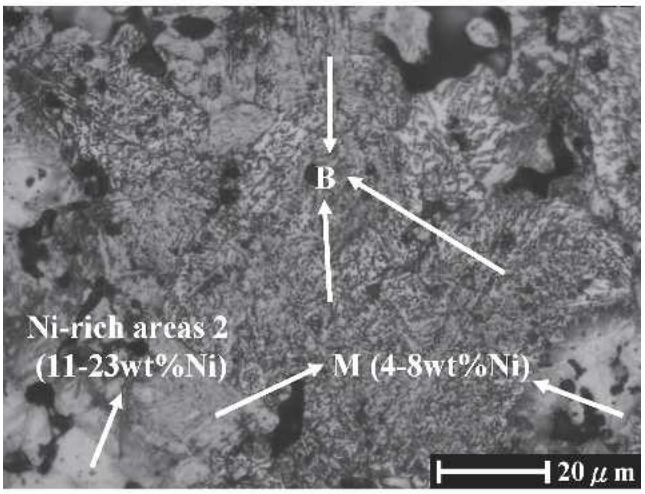

(*b*)

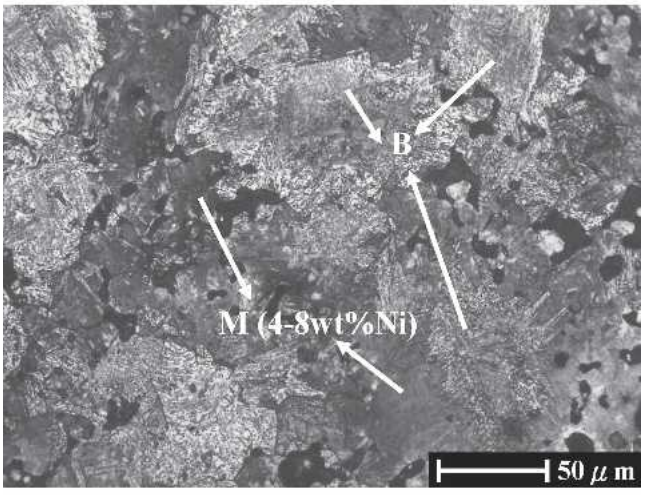

(*c*)

Fig. 5—The microstructure of the diffusion-alloyed Fe-4Ni-1.5Cu-0.5Mo-0.5Cr-0.5C steels that contained 316L powders and were sintered at (*a*) 1120 °C for 30 min, (*b*) an enlarged section of the bainite region, and (*c*) 1250 °C for 1 h.

More fine pearlite and bainite could be found, as shown in Figure 1(b). However, thin Ni-rich areas on the powder surfaces were still present. The mapping of a typical area, as shown in Figure 4, indicated that the Ni was still not uniformly distributed, even after 1250 °C sintering. The Ni content in the powder core was only about 0.1 wt pct.

C. *Microstructure Evolution of Fe-4Ni-1.5Cu-0.5Mo-0.5C + 316L P/M Steels*

Figure 5 shows the typical microstructure of a diffusion-alloyed Fe-4Ni-1.5Cu-0.5Mo-0.5C steel to which was added 3 wt pct 316L powder (material B) after sintering at 1120 °C and 1250 °C. The specimen sintered at 1120 °C, as shown in Figures 5(a) and (b), exhibited mainly two phases. The first one had featherlike microstructures and a hardness value between HV 270 and 360. These results suggested that these areas were bainites. The other area had a hardness value between HV427 and HV586, which is in the hardness range of martensite. A small portion of pearlite was also present. The Ni-rich areas in the pore-rich region and at the periphery region of the iron powder were much less pronounced compared to those of material A, as shown in Figure 1(a). After 1250 °C sintering, the microstructure consisted mainly of bainite and martensite. No soft Ni-rich phases were found. It was also noticed that more pore rounding occurred after 1250 °C sintering. This pore shape change and the density increase also helped to improve the mechanical properties.

To understand the effect of Cr addition on the microstructure changes, the mappings of Cr, Mo, Ni, and Cu for specimens that were sintered at 1000 °C, 1050 °C, 1120 °C, and 1250 °C were examined. Figure 6 reveals that no Mo-rich areas were found after the specimen was sintered at 1000 °C, because Mo has a much faster diffusion rate in Fe compared to those of Cr, Ni, and Cu. In contrast, Cr-rich, Ni-rich, and Cu-rich areas were present, and these were believed to be the original sites of the alloying powder additives. Figure 6 also reveals that pearlite formed at the periphery of the iron powder, indicating that the carbon had diffused into these regions.

After sintering at 1050 °C, the segregation of Ni, Cu, and Cr improved, as shown in Figure 7. The highest local Cr content found in this specimen was only 7.6 wt pct, much lower than the nominal 16.46 wt pct Cr in the as-received 316L powder. This result suggested that the chromium oxide on the 316L powder surfaces, which was a diffusion barrier, was reduced between 1000 °C and 1050 °C in N_2-9 pctH_2 and caused Cr diffusion into the iron matrix. This agreed with previous thermodynamic calculations and experimental results reported by others.[11,12] Since Cr, once reduced, has a higher diffusion rate than Ni, it was more uniformly distributed.[8] It was also noticed that pearlites continued to form due to the large solubility of carbon in iron after ferrite-austenite transformation, as reported in the dilatometer studies by St-Laurent *et al.*[23]

When the specimens were sintered at 1120 °C, the distributions of Ni and Cu, as shown in Figure 8, became more uniform and were significantly improved from those of material A, which did not have Cr additions, as shown in Figure 3. The distribution of Cr was also improved. The quantitative analysis indicated that the Cr contents in the

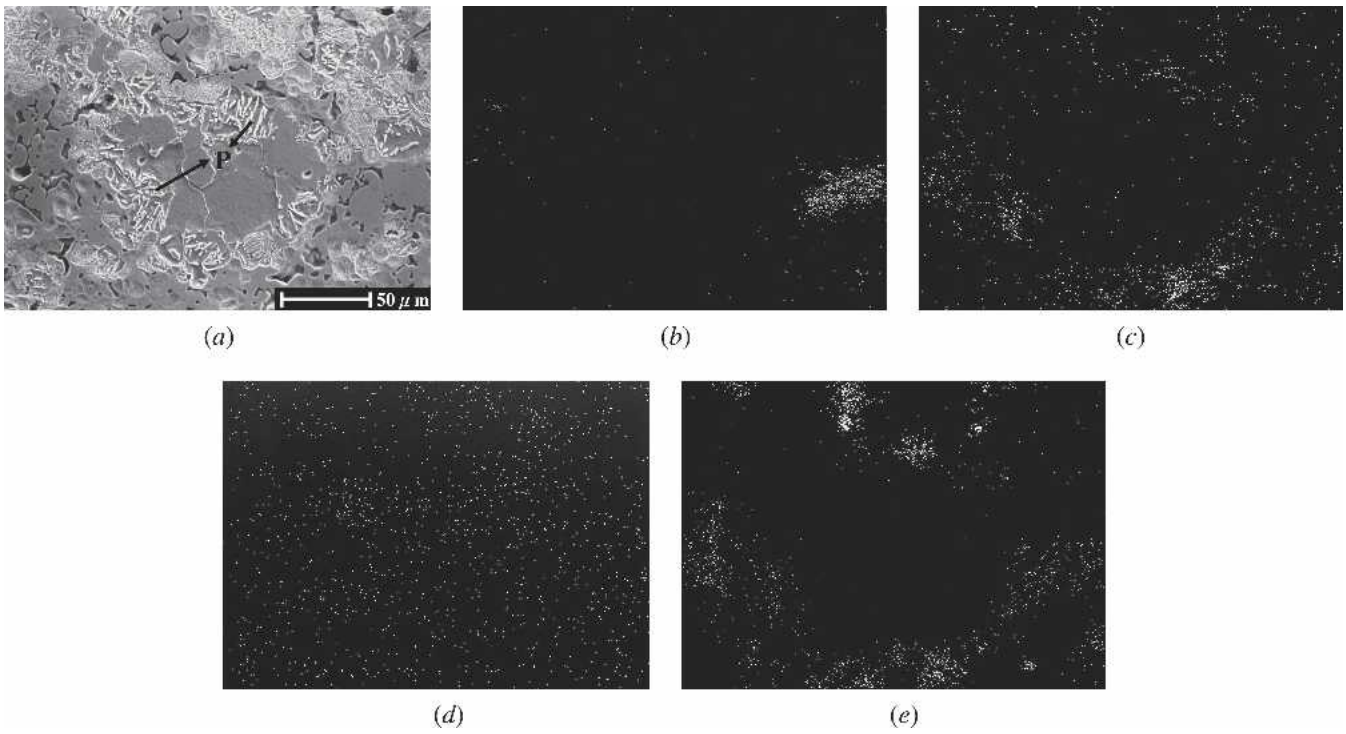

Fig. 6—(*a*) through (*e*) The mappings of Cr (*b*), Cu (*c*), Mo (*d*), and Ni (*e*) in the diffusion-alloyed specimen that was mixed with 316L, showing that most Ni, Cu, and 316L powders remain in the powder form after 1000 °C sintering for 30 min.

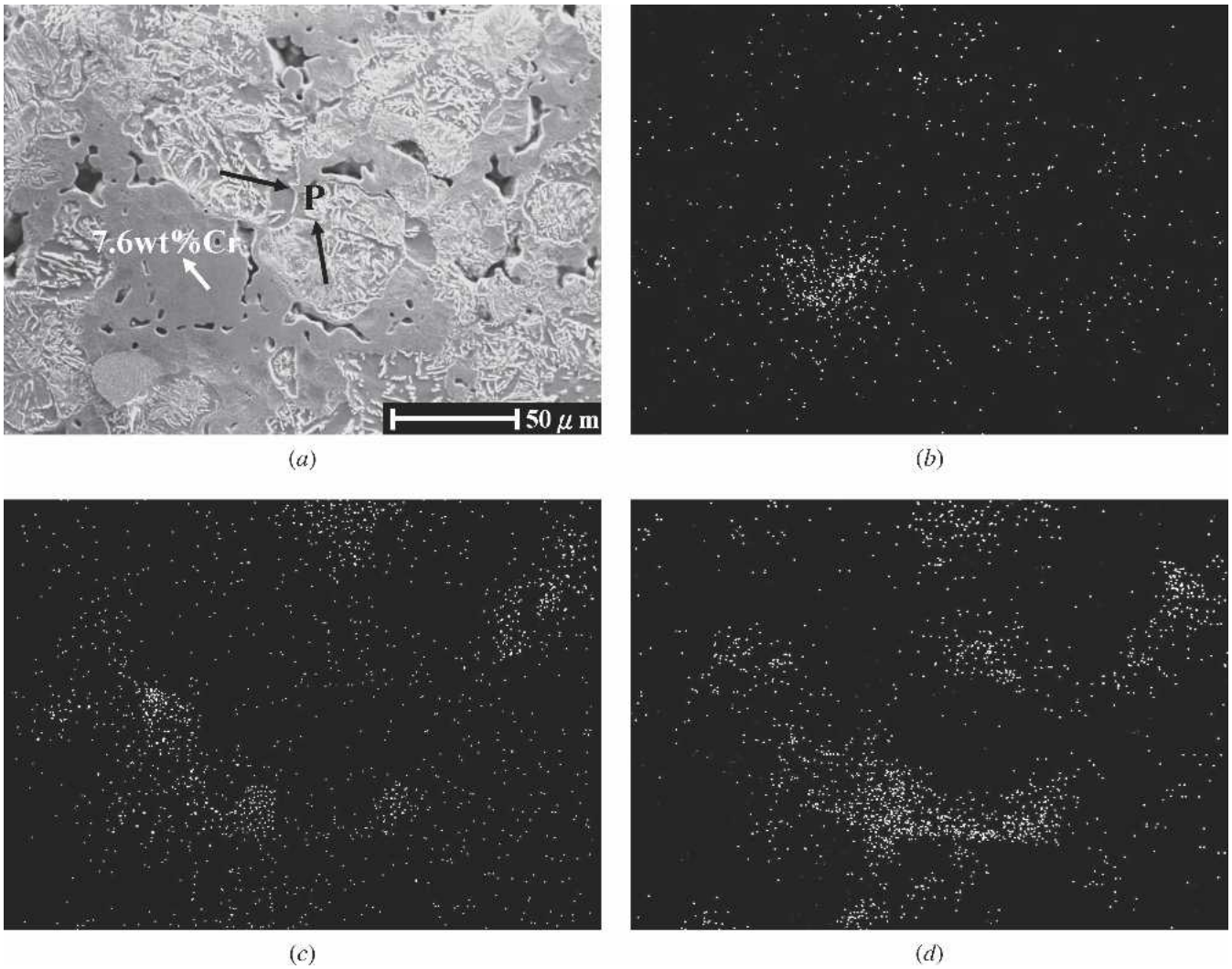

Fig. 7—(*a*) through (*d*) The mappings of Cr (*b*), Cu (*c*), and Ni (*d*) in the diffusion-bonded steel that was mixed with 316L powder, showing that Cr and Cu had diffused into the matrix after 1050 °C sintering for 30 min.

interior and at the periphery of the iron powder were about 0.1 and 1 wt pct, respectively.

The mappings in Figure 9 show that the homogeneity of Cr, Ni, and Cu had been significantly improved after 1250 °C sintering for 1 hour. The Cr content measured using EPMA indicated that the Cr was very uniformly distributed throughout the matrix and was about 0.5 wt pct. The Ni distribution also improved. Its content in the iron powder core increased to about 0.4 wt pct, as compared to the 0.1 wt pct in the similar region for material A.

To further confirm the effect of Cr addition on alloying homogenization, the line scans of C, Ni, Cu, and Cr on typical iron particles that were sintered at 1250 °C were examined. Figure 10(a) shows that the iron powder core contained high C and low Ni, while the surface region contained low C and high Ni. This nonuniform distribution of Ni and C is caused by the strong repelling effect, as reported by Sozinov and Gavrilijuk.[9] Through Thermo-Calc program calculations, they indicated that the presence of Ni or Si in austenite increases the chemical potential of carbon and thus decreases the equilibrium carbon content in the austenite.[24] With a low carbon and high Ni content, no bainite or martensite could be found in these Ni-rich/C-lean areas after cooling. Such inhomogeneous microstructures could still be found, as shown in Figure 1(b), even after 1250 °C sintering. When 316L stainless steel powders were added to introduce 0.5 pct Cr, the differences of Ni and C content between the surface and the core region diminished, as demonstrated in Figure 10(b).

To correlate the microstructures with the mechanical properties presented previously, a CCT graph was constructed, as shown in Figure 11. As indicated by the CCT curves, pearlites, bainites, and martensites should be present in FD-0405 specimens. With the addition of 0.5 pct Cr, the CCT curve shifted to the right side because the multiplying factor of hardenability increased by approximately 2.1 times.[25] As a result, only bainites and martensites would be present when a cooling rate of 0.1 °C/s was employed. These results agreed with the

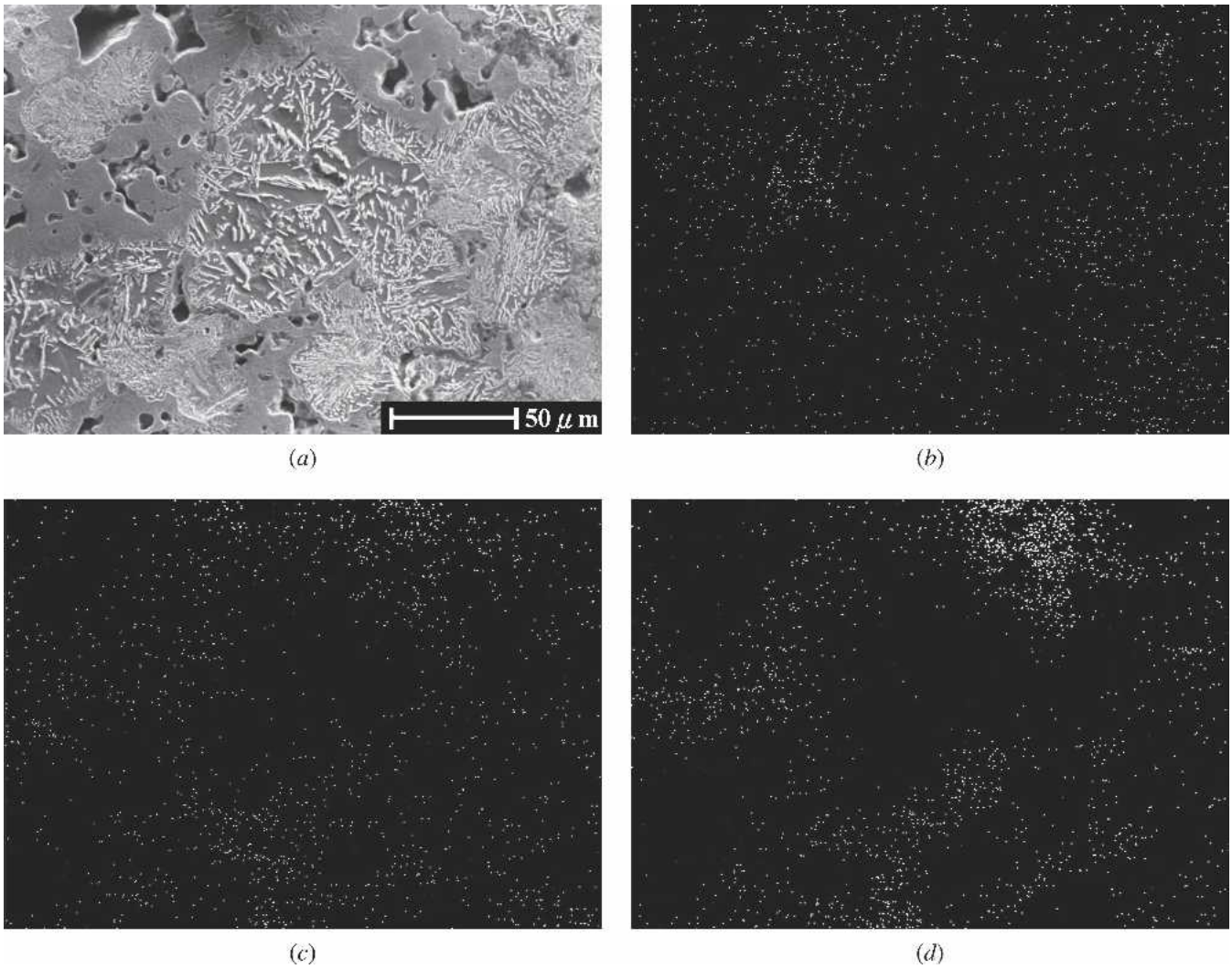

Fig. 8—(*a*) through (*d*) The mappings of Cr (*b*), Cu (*c*), and Ni (*d*) in diffusion-bonded steels mixed with 316L powder after 1120 °C sintering for 30 min.

microstructures observed and the mechanical properties attained.

The preceding observations suggest that the presence of Cr, which is a strong carbide former, can help improve the distribution of carbon and nickel in the matrix. It also increases the multiplying factor of hardenability. Thus, more bainites and martensites form, and the soft Ni-rich areas are eliminated. With these encouraging results from adding Cr into Ni-containing specimens, it should be plausible to use a prealloyed Fe-Cr powder as the base powder to further enhance the beneficial effect of Cr addition. It is believed that, with the Cr being uniformly distributed in the prealloyed powder, the homogenization of C and Ni and the mechanical properties should be further improved. Work on this subject is now under way.

IV. CONCLUSIONS

The addition of 0.5 wt pct Cr, introduced in the 316L powder form, improves the alloy homogeneity of diffusion-alloyed Fe-4Ni-1.5Cu-0.5Mo-0.5C P/M steels. When 1250 °C sintering is employed, the ultimate tensile strength of the tensile bar in the as-furnace-cooled condition increases from 626 to 801 MPa, a 28 pct increase. The microstructure of the sintered steel without Cr additions shows that Ni is the least homogenized element and is concentrated in the pore-rich regions or in the surface region of iron powders. The presence of Ni in these areas reduces the carbon content and forms soft Ni-rich phases, which become the most likely sites of crack initiation and cause failures during mechanical testing. This problem is solved with the addition of Cr, particularly in combination with the 1250 °C high-temperature sintering. The presence of Cr eliminates soft Ni-rich areas. When 1120 °C is used, some residual Ni-rich areas are still present. However, the carbon content is higher than that of Cr-free compacts due to the lessening of the repelling effect between Ni and C. With more homogenized Ni and C and thus more bainite and martensite present, the tensile strength and hardness are improved.

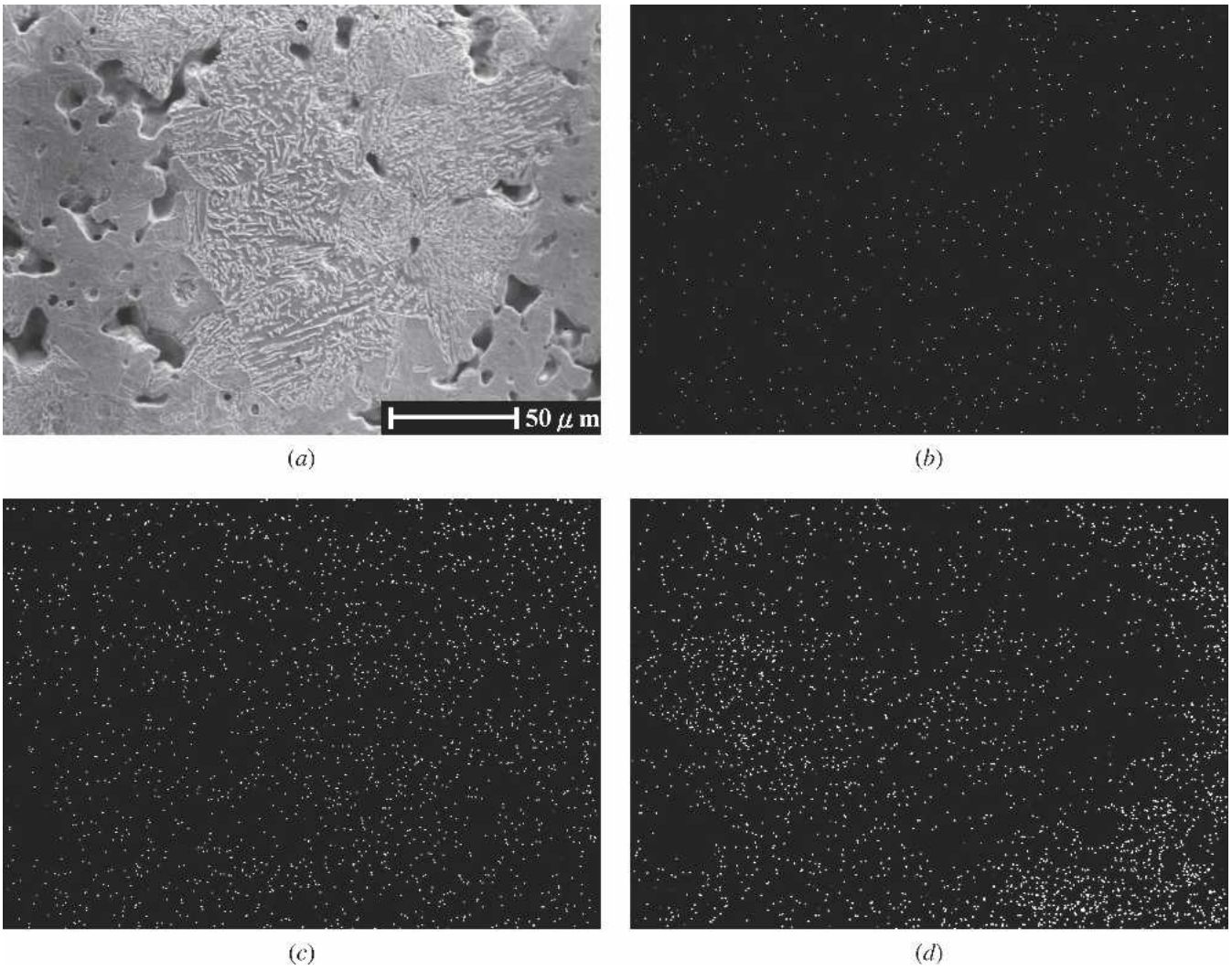

Fig. 9—(*a*) through (*d*) The mappings of Cr (*b*), Cu (*c*), and Ni (*d*) in diffusion-bonded steels mixed with 316L powder after 1250 °C sintering for 1 h.

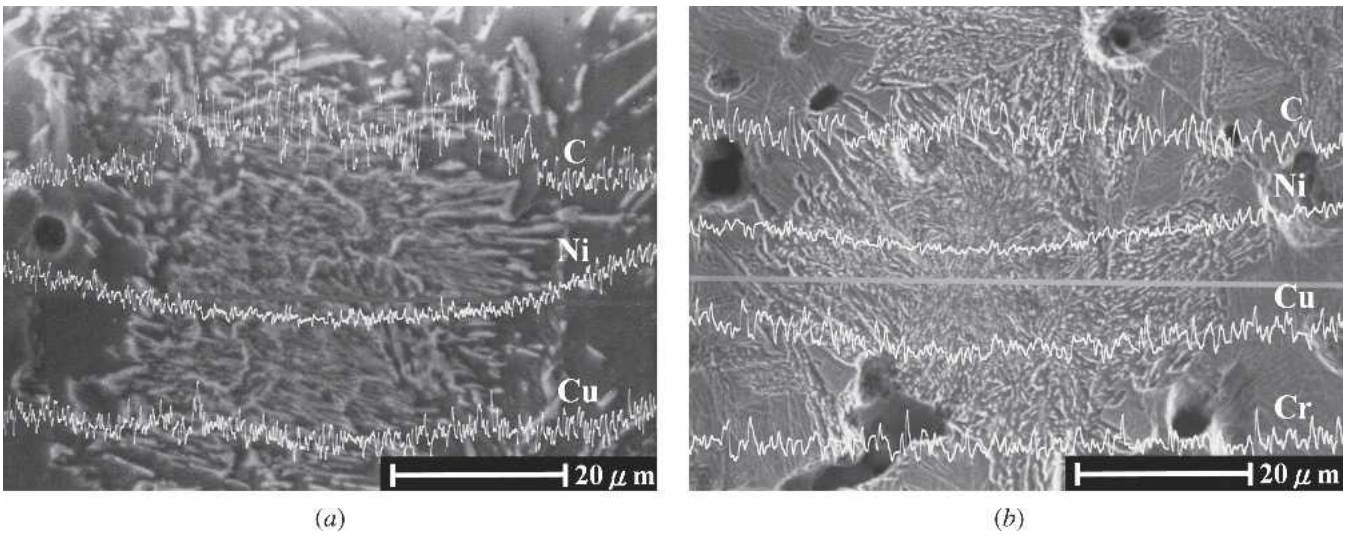

Fig. 10—The line scans of Ni, Cu, and C around a typical powder for (*a*) FD-0405 sintered steel and (*b*) an FD-0405 specimen mixed with 3 pct 316L powder after 1250 °C sintering, showing that Cr addition helps the homogenization of alloying elements, particularly the carbon.

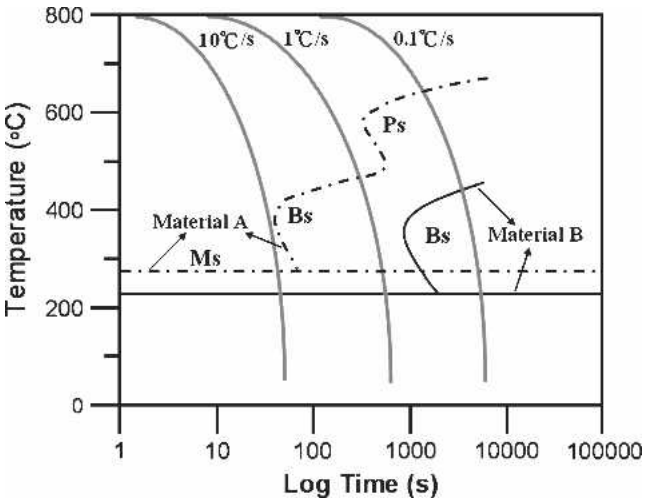

Fig. 11—The CCT graph of FD-0405 and FD-0405 with the addition of 3 pct 316L powders.

ACKNOWLEDGMENT

The authors thank the Hoeganaes Corp. for their support of this project under Contract No. 91-S-A57.

REFERENCES

1. R. Haynes: *Powder Metall.*, 1989, vol. 32 (2), pp. 140-46.
2. M. Khaleghi and R. Haynes: *Powder Metall.*, 1985, vol. 28 (4), pp. 217-23.
3. S. Berg: *Adv. Powder Metall. Part. Mater.*, compiled by C.L. Rose and M.H. Thibodeau, MPIF, Princeton, NJ, 1999, vol. 2 (part 7), pp. 163-69.
4. N. Douib, I.J. Mellanby, and J.R. Moon: *Powder Metall.*, 1988, vol. 32 (3), pp. 209-14.
5. E. Dudrova, M. Kabatova, and M. Kupkova: *Kov. Mater.*, 2002, vol. 40, pp. 24-33.
6. C. Verdu, S. Carabajar, G. Lormand, and R. Fougeres: *Mater. Sci. Eng.*, 2001, vols. 319A–321A, pp. 544-49.
7. S. Carabajar, C. Verdu, A. Hamel, and R. Fougeres: *Mater. Sci. Eng.*, 1998, vol. 257A, pp. 225-34.
8. R.C. Weast and M.J. Astle: *CRC Handbook of Chemistry and Physics,* 61st ed., CRC Press, Boca Raton, FL, 1980–1981, p. F-65.
9. A.L. Sozinov and V.G. Gavrilijuk: *Scripta Mater.*, 1999, vol. 41 (6), pp. 679-83.
10. K. Kanno and Y. Takeda: *Adv. Powder Metall. Part. Mater.*, compiled by V. Arnhold, C.L. Chu, W.F. Jandeska, and H.I. Sanderow, MPIF, Princeton, NJ, 2002, vol. 2 (part 13), pp. 14-22.
11. P. Ortiz and F. Castro: *Powder Metall.*, 2004, vol. 47 (3), pp. 291-98.
12. B. Lindqvist and K. Kanno: *Adv. Powder Metall. Part. Mater.*, compiled by V. Arnhold, C.L. Chu, W.F. Jandeska, and H.I. Sanderow, MPIF, Princeton, NJ, 2002, part 13, pp. 278-90.
13. K.S. Hwang and M.Y. Shiau: *Metall. Mater. Trans. B*, 1996, vol. 27B, pp. 203-11.
14. P.F. Stablein, Jr. and G.C. Kuczynski: *Acta Metall.*, 1963, vol. 11 (3), pp. 1327-37.
15. J. Puckert, W.A. Kaysser, and G. Petzow: *Int. J. Powder Metall.*, 1984, vol. 20 (4), pp. 301-10.
16. S.J. Jamil and G.A. Chadwick: *Powder Metall.*, 1985, vol. 28 (2), pp. 65-71.
17. H. Kuroki, G. Han, and K. Shinozaki: *Int. J. Powder Metal. Powder Technol.*, 1999, vol. 32 (2), pp. 57-62.
18. R.L. Lawcock and T.J. Davies: *Powder Metall.*, 1990, vol. 33 (2), pp. 147-50.
19. C.T. Huang and K.S. Hwang: *Powder Metall.*, 1996, vol. 39 (2), pp. 119-23.
20. N. Chawla and X. Deng: *Mater. Sci. Eng.*, 2005, vol. 390A, pp. 98-112.
21. W.A. Spitzig, R.E. Semlser, and O. Richmond: *Acta Metall.*, 1988, vol. 36 (5), pp. 1201-11.
22. R.J. Bourcier, D.A. Koss, R.E. Smelser, and O. Richmond: *Acta Metall.*, 1986, vol. 34 (12), pp. 2443-53.
23. S. St-Laurent, P. Lemieux, and S. Pelletier: *Adv. Powder Metall. Part. Mater.*, compiled by W.B. James and R.A. Chernenkoff, MPIF, Princeton, NJ, 2004, part 10, pp. 145-59.
24. D.A. Porter and K.E. Easterling: *Phase Transformations in Metals and Alloys,* 2nd ed., CRC Press, Boca Raton, FL, 1992, pp. 96-98.
25. W.F. Smith: *Structure and Properties of Engineering Alloys,* 2nd ed., McGraw-Hill Co., New York, NY, 1993, pp. 136-37.